UGC-SVU CENTRE FOR MST RADAR APPLICATIONS
SV UNIVERSITY, TIRUPATI – 517 502
PROGRESS REPORT DURING THE PERIOD 2017-2022.

***Recognized as a National Facility in the Country by the University Grants Commission, New Delhi.**

Prof. S. Vijaya Bhaskara Rao
Director

Department of Physics
S. V. U. College of Sciences
S. V. University
Tirupati - 517502

The UGC-SVU Centre was established in the year 1996 and is being actively supporting the user scientific community visiting from all over the country for the past 26 years.

Organization

- I U A C
- I U C A A
- UGC DAE CSR
- C E C
- INFLIBNET
- IUCIS
- NAAC
- Chairman
- Vice-Chairman
- Secretary
- Financial Advisor
- Additional Secretary-I
- Additional Secretary-II
- Consultants
- Joint Secretaries
- Deputy Secretaries
- Under Secretaries
- Telephone Directory
- UGC Regional Offices
- Education Officers
- National Facilities

National Facilities

The UGC has established 4 National Facilities Centre in the selected universities as per details given below:-

1. Western Regional Instrumentation Centre, Mumbai, Mumbai University
2. M.S.T. Radar Facilities, Sri Venkateshwar University, Tirupati
3. Inter University Centre for Humanities and Social Sciences IUCHSS, Indian Institute of Advanced Study, Shimla
4. Crystal Growth Centre, Anna University, Madras

1. **Western Regional Instrumentation Centre, Mumbai**

This Centre was established by University Grants Commission in 1978 under the administrative control of Mumbai University with the objective to provide training to USIC staff and students for proper use and maintenance of instruments conducting advanced study programmes such as workshops, seminars for teachers, Research workers from University, National Laboratories and industries etc.

Recommendations of the XI Plan Review Committee.

More Info »

2. **M.S.T. Radar Facilities, Sri Venkateshwar University, Tirupati**

The University Grants has established a centre for MST Radar application in the Physics Department SU University, Tirupati in 1990 to utilize the National MST Radar facilities created at Gadanki by the Researchers and Scientists in Indian Universities.

Recommendations of the XI Plan Review Committee.

More Info »

3. **Inter University Centre for Humanities and Social Sciences IUCHSS, Indian Institute of Advanced Study, Shimla**

The main objectives of the Centre are to invite teachers from universities and colleges to the institute as associate of the IUC, organise "Research Seminars" for researchers and young teachers in University and Colleges and to organize "Study weeks" for discussing important problems of National and international interest.

Recommendations of the XI Plan Review Committee.

More Info »

4. **Crystal Growth Centre, Anna University, Madras**

This centre was established in 1982 with the following objectives.

a. To develop facilites for growth and growth and characterization of crystal of technological and industrial importance.

b. To bridge the gap between needy industries and Lab. Res.

c. To cater the needs of various institutions in India with regard to requirements of special crystal for Research etc.

Recommendations of the XI Plan Review Committee.

More Info »

Historical Backdrop:

To create scientific awareness about the potential use of the sophisticated radar and other instrumentation facilities for advanced research in the area of atmospheric sciences and to attract bright and young researchers to utilise the MST Radar, Lidar and other co-located Facilities available at NARL, Gadanki; University Grants Commission (UGC) has established an UGC-SVU Centre at S.V. University, Tirupati, to serves as a common platform for the University system in India for the exchange of scientific knowledge and the centre is accessible to scientist and researcher from Indian Universities working in the area of Atmospheric Sciences.

Objectives& Salient Features:

- UGC-SVU Centre is accessible to scientists and researchers from Indian University working in the area of Atmospheric Sciences.
- UGC-SVU Centre provides necessary facilities for research and basic computational and other support for carrying out such research.
- UGC-SVU Centre offers a forum for exchange visits in the area of Atmospheric Science so that the Indian Atmospheric Scientific Community will benefit from such co-operation.
- UGC-SVU Centre helps in training postgraduate students and research fellows in a number of challenging tasks in the thrust area of Atmospheric Physics.
- UGC-SVU Centre assists in coordinating the experimental programme in the area of Atmospheric Dynamics using MST Radar and other co-locatable instrumentation facilities with special reference to the location of these facilities.
- UGC-SVU Centre organizes comprehensive National data bank/archrivals in specified areas of Atmospheric Sciences especially out of the large volume of processed data obtained from MST Radar and other collocated facilities.
- UGC-SVU Centre helps in the generation and updating models for the middle atmosphere over Indian latitudes. Use of such models and data in turn will help in forecasting and prediction by IMD and other concerned national organizations.

Major Facilities Available:

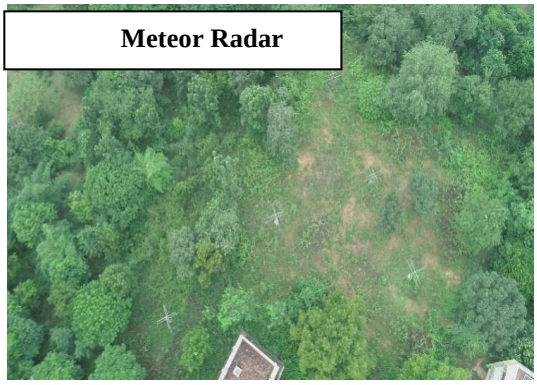

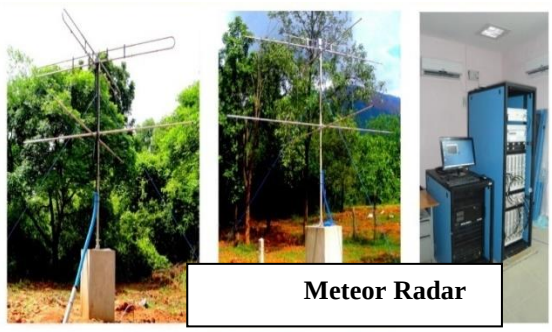

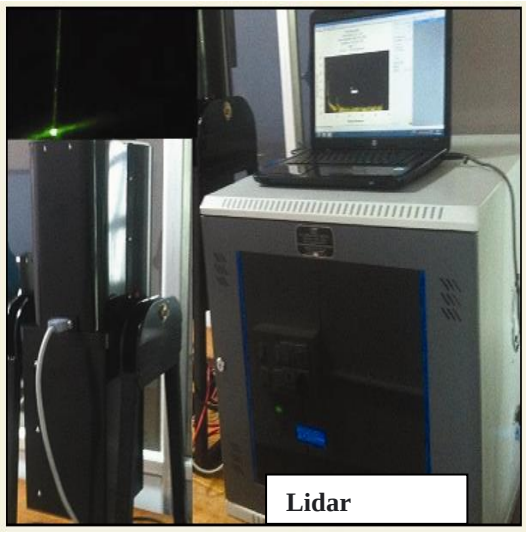

Grants Recieved:

Duration	Grants
2016 - 2017	**39,90,000.00**
2017 - 2018	**12,17,872.00**
2018 - 2019	**28,07,128.00**
2019 - 2020	**4,50,000.00**
2020 - 2021	**11,25,000.00**
2021 - 2022	**4,30,000.00**

International collaboration:

- Dr. Brian J. Harding - Space Sciences Laboratory, University of California, Berkeley, CA, USA.
- Dr. Jorge L. Chau - Leibniz Institute Of Atmospheric Physics at the University Of Rostock, Kuhlungsborn, Germany.
- Dr. Jonathan J. Makela – Department Of Elecrical and Computer Engineering,University Of Illinois at Urbana-Champaign, Urbana, IL, USA.
- Dr. Christian Adami – Atmospheric Radar Systems, SA, 5031, Australia.

National Collaborations:

- National Atmospheric Research Laboratory, Gadanki.
- Space Physics Laboratory, Trivandrum.
- Pune University, Pune.
- Physical Research Laboratory, PRL, Ahmadabad.
- IITM, Pune.

The following members (Faculty, Scientists and Research scholars) have visited UGC-SVU Centre during 2017-2022.

1. Dr. G. Yellaiah, Professor, Department of Astronomy, Osmania University, Hyderabad.
2. Mr.HerambGaikwad, Research scholar, Department of Physics Shivaji University, Kolhapur.
3. C.B.R. Lakshmi, Assistant Professor, VBIT, Aushapur, GhatkewarMandam, R.R. Distric.
4. Prof. B. Surya Prakash Rao, Dept. Geo- Engineering, Andhra University, Viskhapatnam.
5. Prof. Siddeswar, Dept. of Mathematics, Bangalore University, Bangalore.
6. Dr. G. Mrudula, Scientist- D, CSIR- National Aerospace Laboratory, Bangalore.
7. Dr. A. Ramesh Babu Naidu, Associate Professor, Pondicherry University, Pondicherry.
8. Prof. S. Mohan, Indian Institute of Science (IISc), Bangalore.
9. Dr.PrashantBakshe, Associate Professor, Department of Mechanical Engineering VBIT, Hyderabad.
10. Prof. CK. Haridas, Dy. GMT Telecom (Rtd), Founder chairman IETE, Palakkad.

11. Dr. K. Madhu Chandra Reddy, Scientist, Indian Institute of Tropical Meteorology (IITM), Pune.
12. Prof. NileshKasat, Spine College of Engineering, Amravati, Maharashtra.
13. Ms. Dolly More, Research Assistant, M.Sc Atmospheric Science, Department of Atmospheric and Space Sciences, SavitribaiPhule Pune University, Pune.
14. Dr. K.V. Swamy, Dy. Director, Employment Department, Hyderabad.
15. Y. Subramanyam, Section officer, IGNOU, Pune.
16. Dr. Sanjay Sengupta, editor, JSIR, New Delhi.
17. Sri Y. Subramanyam, Section officer, IGNOU, Pune.
18. Dr. N. V.P. Kiran Kumar, Scientist - SE, Space Physics Laboratory, Dept. of Space, Trivandrum.
19. Dr. Ch. Kanaka Rao, Department of Physics, Andhra University, Visakhapatnam.
20. Prof. K. Niranjan, Dept. of Physics, Andhra University, Visakhapatnam.
21. Prof. B. Surya PrakashRao, Emeritus Professor, Andhra University, Viskhapatnam.
22. Prof.Siddeswar, Dept. of Mathematics, Bangalore University, Bangalore.
23. Mrs. M. Amutha, PS to Director, Research SRM University, Chennai.
24. Miss. AnkitaShitole, Junior Research Fellow, Department of Atmospheric and Space Sciences, SavitribaiPhule Pune University, Pune.
25. Dr. R. Suresh, Director, Airport Met Office, Indian Meteorological Department, Technical Building, Air Traffic Services, Meenambakkam, Chennai.
26. Dr. Grandhi Kishore Kumar, Assistant Professor, Dept. of Atmospheric and Space Science, SavitribaiPhule Pune University, Pune.
27. Dr. M. M Ali,Emiratus Scientist/ Professor, Pune University, Pune.
28. Dr.Onkar Bharat Gurav, Assistant Professor, Dept. of Physics, Shivaji University, Kolhapur.
29. Sri K.G. Kumar, Former Director, VisvesvarayaIndusrial and Technological Museum, Bangalore. Prof. T. SubbaRao, Dept. of Physics, S.K. University, Ananthapuramu.
30. Dr. K. Chenna Reddy, Assistant Professor, Dept. of Astronomy, Osmania University, Hyderabad
31. Prof. K. Niranjan, Dept of Physics, Andhra University, Visakhapatnam.
32. Prof. CA.Babu, Dept. of Atmospheric Sciences, Cochin University, Cochin.
33. Dr.Naresh Krishna Vissa, Assistant Professor II, Dept of Earth and Atmospheric
34. Science, National Institute of Technology, Rourkela.
35. Dr.Naresh Krishna Vissa, Assistant Professor II, Dept of Earth and Atmospheric Science, National Institute of Technology, Rourkela.
36. Miss. A. Veekshitha, B.Tech (III), Electronic & Telecommunication, Symbiosis Institute of Technology, Pune.
37. Mr. S. Ravindran, Scientist - G, Division Head, Prof UR Rao Centre, ISRO,

Bangalore.

38. Dr. G. Mrudula, Senior Scientist, CSIR- National Aerospace Laboratory, Bangalore.
39. Dr. M.M Ali, Emiratus Scientist, NRSC, Hyderabad.
40. Dr. N. NanajiRao, PDF, Dept. of Meteorology, Andhra University, Visakhapatnam.
41. Mr. Philip Daniel Maret, O/o Director, ESSO- National Centre for Earth Sciences Studies, Trivandrum.
42. Dr. S. Murugappan, Rtd.,Chief (Geophysics), Subansiri Lower Project, National Hydroelectric Power Corporation Limited, Gerukamukh, Assam.
43. Prof. D. Dinakar, Dept of Physics, NIT, Warangal.

Ph.D. degrees awarded using the facility:

1. Mr.PeddapatiPavanchaitanya on the topic "**LOW LATITUDE LONOSPHERICELECTRODYNAMISS: OBSERVATIONS AND MODELLING"**, Dr. A.K. Patra&Prof.S. Vijaya Bhaskara Rao, April, 2017.

2. Ms.Sreekala P.P. on the topic "**NORTHEAST MONSOON RAINFALL VARIABILITY OVER SOUTH PENINSULAR INDIA AND ITS PREDICTABILITY USING IPCC-AR5 MODELS**", Prof. S. Vijaya Bhaskara Rao&Dr. M. Rajeevan, February, 2017.

3. Mr.Amitt Kumar Pandit, on the topic "**CLIMATOLOGY OF CIRRUS CLOUDS OBSERVED USING GROUND –BASED AND SPACE –BORNE LIDARS OVER A TROPICAL STATION IN SOUTH INDIA"**Dr. A. Jaya raman& Prof. S. Vijaya Bhaskara Rao February, 2017.
4. Mrs. M. Pramitha on the topic **"IDENTIFICATION OF GAVITY WAVE SOURCES IN THE TROPICAL REGION USING RAY TRACTING TECHNOLOGY,"** Dr. M. VenkataRatnam**&**Prof. S. Vijaya Bhaskara Rao, June, 2017.

5. Mrs. Amara Jyothi on the topic **"A STUDY ON RAIN MICROPHYSICS USING POLARIMETRIC RADARS: SIMULATIONS AND OBSERVATIONS,"** Dr. T. Narayana Rao& Prof. S. Vijaya Bhaskara Rao, June, 2017.

6. Mr. U. Umakanth on the topic **"SIMULATION OF INTRASEASONAL OSCILLATIONS OF INDIAN SUMMER MONSOON: A STUDY USING REGIONAL CLIMATE MODELS",** Dr.Amit P kesarkar**&**Prof.S. Vijaya Bhaskara Rao, September, 2017.

7. Mr. S. KarunaSaagar on the topic **"STUDIES ON RAINSTROMS OVER INDIA: OBSERVATIONS AND PREDICTABILITY"** Dr.Rajeevan&Prof.S. Vijaya Bhaskara Rao, November, 2017.

8. Mrs. Veda Vathi on the topic **"SOLAR INFLUENCE IN THE MIDDLE ATMOSPHERE OBSERVED USING METEOR/ MF RADAR AND RE- ANALYSIS DATASETS",**Prof. S. VijayaBhaskara Rao &Dr. M. VenkatRatnam, January, 2018.

9. Mrs.Y.Sulochana on the topic "**RAINFALL ESTIMATION AND PRDCIPITATION STUDIES FOR RAIN ARRENUATION**", Prof. S. Vijaya BhaskaraRao, March, 2018.

10. Ms. S. Jyothi, "**STUDIES ON THE SPATIAL AND TEMPORAL VARIABILITY OF PRECIPITATION AND TEMPERATURE OVER INDIA" December, 2018,** Prof. S. Vijaya Bhaskara Rao.

11. K. Swapna (M.Phil) on the topic **"Indoor Propagation Models for Mobile Communications**" January, 2018.

12. Mr. P. Prasad on the topic **"ROLE OF METEOROLOGY AND DYNAMICS ON THE SURFACE AND ELEVATED AEROSOL LAYERS OVER PENINSULAR INDIA"** Prof. S. VijayaBhaskaraRao, February, 2020.

13. Mrs. P. Mohanamanasa on the topic **"STUDIES ON THE MAGNETICALLY CONTROLLED DENSITY STRUCTURES IN THE MARTIAN IONOSPHERE"** Prof. S. Vijaya BhaskaraRao, August, 2020.

14. Mrs.Seshu Mani on the topic **"STUDY OF MAGNETIC AND ELECTRICAL PROPERTIES OF MICROCONTROLLER EMBEDDED SYSTEM BASED VISCOMETER"** Prof. S. Vijaya Bhaskara Rao, August, 2020.

15. Mr. A. Lakshmi Kanth, on the topic **"PERFORMANCE OPTIMIZATION OF WRF SHORT-RANGE WEATHER PREDICTION SYSTEM OVER THE INDIAN REGION: SENSITIVITY ANALYSISON COMPUTATIONAL AND OBSERVATION ASSIMILATION ASPECTS"** Prof. S. Vijaya Bhaskara Rao, February, 2021.

Salient features of work done:

(i) Mesospheric Studies

We have utilized the Gadanki MST Radar and Rayleigh LIDAR to understand the vertical coupling between the lower atmosphere and mesosphere through the short-period gravity waves (GWs). The short-period GWs (20 min to 2 h) are notice both in the troposphere and in the mesosphere during the deep convection. During the convection, the large vertical velocities (>5 m/s) and significant variations in the momentum flux (~3 m/s2) are noticed in the troposphere and higher fluxes (~45 m2/s2) are evidenced in the mesosphere. The observations suggest the vertical coupling between the lower and middle atmosphere during convection.

The vertical flux of the horizontal momentum of GWs of periods in the range 20 min. to 2h is investigated in the mesosphere using the MST Radar winds. The emphasis is made on the variability of zonal and meridional momentum fluxes in the mesosphere and possible reasons for the variability of fluxes during MTI. It is observed that raise in momentum fluxes of ~7 m2/s2 in the eastward flux and ~10 m2/s2 in southward flux at mesospheric altitudes during the MTI. The gravity wave (GW) analysis using the LIDAR temperature profiles indicate the connection between GW breaking at mesosphere altitudes and temperature inversion and thus the turbulence caused mesospheric echoes. The study suggests the prospect of coupling between stratosphere and mesosphere during the MTI.

The various occurrence characteristics of day and night tropical (10^oN-15^oN, 60^oE-90^oE) mesospheric inversion layers (MILs) are studied using TIMED-SABER (Thermosphere-Ionosphere-Mesosphere Energetics and Dynamics-Sounding of the Atmosphere using Broadband Emission Radiometry) satellite data products of kinetic temperature, volume mixing ratios of O, H, and O_3, volume emission rates of $O_2(^1\Delta)$and OH (1.6**μ**m channel), chemical heating rates due to seven dominant exothermic reactions among H, O, O_2, O_3, OH, HO_2, and CO_2 cooling rates for the year 2011. Although both dynamics and chemistry play important roles, the present study mainly focuses on the chemical processes involved in the formation of day and night MILs. It is found that the upper level height of daytime (night time) MIL descends (ascends) from ~88 km (~80 km) in winter to ~72 km (~90 km) in summer. The day and night inversion amplitudes are correlated with total chemical heating rates and CO_2 cooling rates and they show semi annual variation with larger (smaller) values during equinoxes (solstices). The daytime (night time) inversion layers are predominantly due to the exothermic reaction, Rs: $O+O+M\rightarrow O_2+M$ and R6:$O+O_2+M \rightarrow O_3+M$ (R3: $H+O_3\rightarrow OH+O_2$). In addition, the CO_2 causes large cooling at the top and small heating at the bottom levels of both day and night MILs. In the absence of dynamical effects, the chemical heating and CO_2 cooling jointly contributes for the occurrence of day and night MILs.

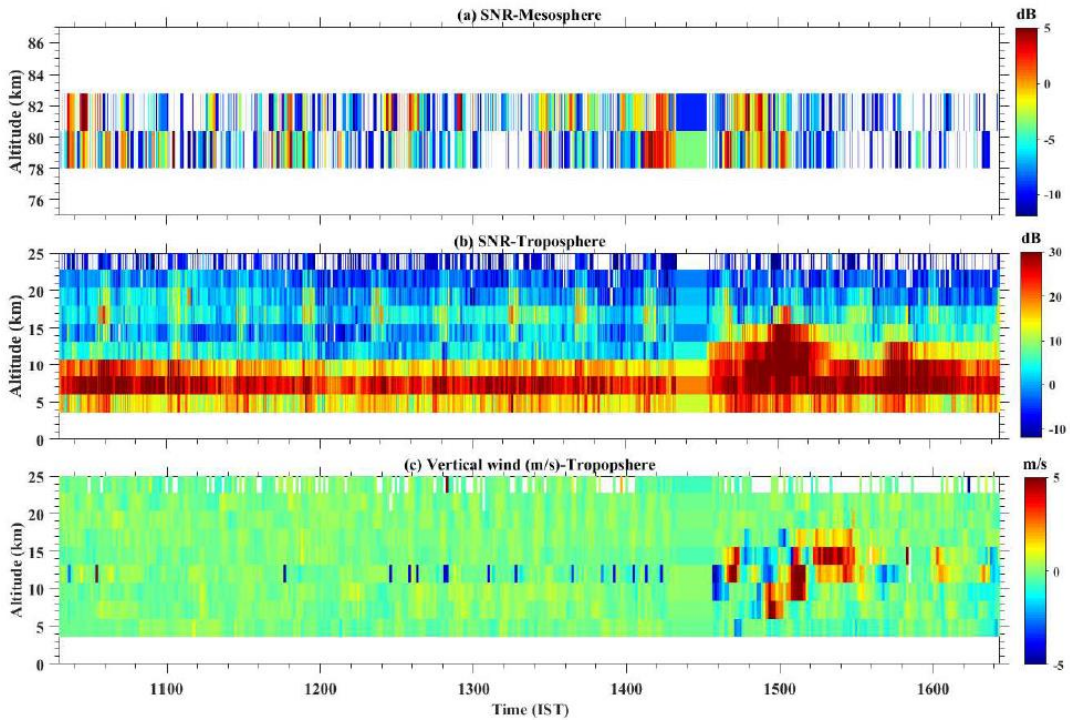

Fig 1. (a) Time-Altitude of signal-to-noise ratio (SNR) observed in the mesosphere. (b) same as (a) but in the troposphere. (c) Time-Altitude plot of vertical wind observed in the troposphere

(ii) Modelling of rain-induced propagation effects, for Earth-space links operating above 10 GHZ.

Rain rate and rain attenuation predictions are one of the most important steps to be considered when analyzing satellite communication links at the Ku and Ka bands. Rain rate distributions are calculated from the global data sets of Tropical Rainfall Measuring Mission (TRMM) and Global Precipitation Climatology Project (GPCP) for six rainfall homogeneous regions of India. The rain rate distributions are estimated from the monthly accumulations of TRMM and GPCP for the years 1998-2010. The estimated rain rate distributions are compared with the standard ITU-R P.837-5 (International Telecommunication Union-for Radio wave propagation) and observed relative errors are also given. The specific rain attenuation calculated at 0.01% & 0.001% probabilities of exceedance in an average year for different frequencies are also presented for the six homogeneous regions of India.

Cumulative distributions of rain rate values in 6 regions over India, the highest rain rate values, are seen in the NE region, the minimum rain rate values in the NW region. Bikaner shows the lowest rain rate value in TRMM and GPCP data sets. The relative error in TRMM and GPCP data sets are compared to the ITU-R 837.5. We observed that the GPCP gives good rain rate estimation in Central North East (CNE), North East (NE) and Peninsular regions (PS). West Central (WC) region TRMM gives the good rain rate estimation.

The evaluation of rain rate value is the first step for the prediction of specific rain attenuation. Using the power law relationship in ITU-R Model K, and α value are used for the

determination of specific rain attenuation. Observations indicate maximum specific attenuation in the NE region over Cheerapunji at 0.001% of the time, and minimum attenuation of 21.988 dB/km in Bikaner at 0.01% for 50 GHz frequency in the NW region. Rain attenuation and rain rate distribution are found to exhibit similar characteristics over the six homogeneous regions of India.

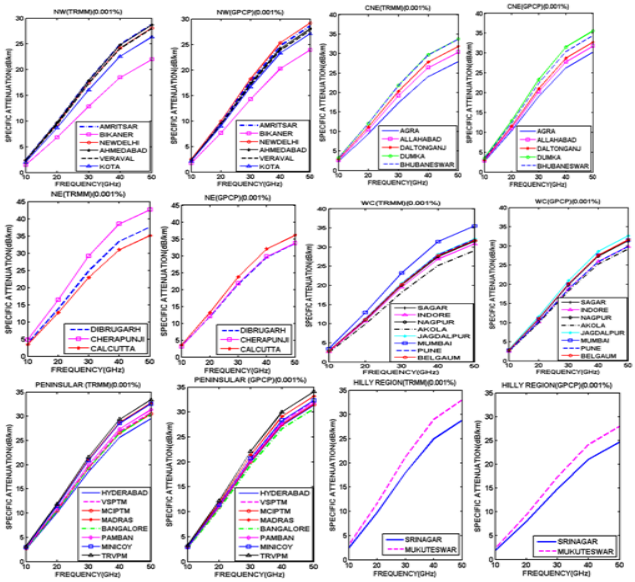

Fig. 2. Specific Attenuation for over all 6 regions at 0.001% of Exceedance

(iii) Monitoring Atmospheric Aerosols and Analyzing their Impacts on Climate

The existence of elevated aerosol layer is common over India during monsoon season. Though its sources are well explained through long-range transport, its formation and maintenance is not explained to date. The formation and maintenances of an elevated aerosol layer, starting from ~2 km and extending up to ~5.5 km noticed is explained using two nearby lidars located in peninsular India. Existence of no strong local source. The low level jet (LLJ) from Arabian Sea persisting between 2 and 3 km is the mail mechanism suggesting strong role of dynamics in the formation of these elevated layers. Persistent strong shears existing between LLJ and tropical easterly jet during this season restrict the up-liftment of aerosols to the higher altitudes. Observed features are explained in the light of dynamics, meteorology and long-range transport.

The present work concerns with a detailed study of the validation of the MODerate Resolution Imaging Spectroradiometer (MODIS) and model products, and investigates the spatial and temporal variations in the correlation coefficient of the validation results obtained from the analysis of **AE**rosol **RO**botic **NET**work (AERONET) sun-sky radiometer data archived at Pune during 2005-2015. Combining the confidence intervals and prediction levels, the ground-based AERONET Aerosol Optical Depth (AOD) at 550nm and Precipitable Water Vapour (PWV) have been used to validate the MODIS, model AOD (550nm) and PWV (cm) observations. The correlation coefficients (r) of AOD for the linear regression fits are 0.73, 0.75, and 0.79, and of PWV are 0.88, 0.89, 0.97 for Terra, Aqua, and model simulations, respectively. Month-to-month/Seasonal variation of AOD (550nm) and PWV observations of satellite and model

observations are also compared with AERONET observations. Additionally, various statistical metrics, including the Root Mean Square Error (RMSE), Mean Absolute Error (MAE), and Root Mean Bias (RMB) values were calculated using AERONET, satellite, and model simulations data. Furthermore, a frequency distribution of AOD (550nm) and PWV observations are studied from AERONET, satellite, and model data. The study emphasizes that the globally distributed AERONET observations help to improve the satellite retrievals and model predictions to enrich our knowledge of aerosols and their impact on climate, the hydrological cycle, and air quality.

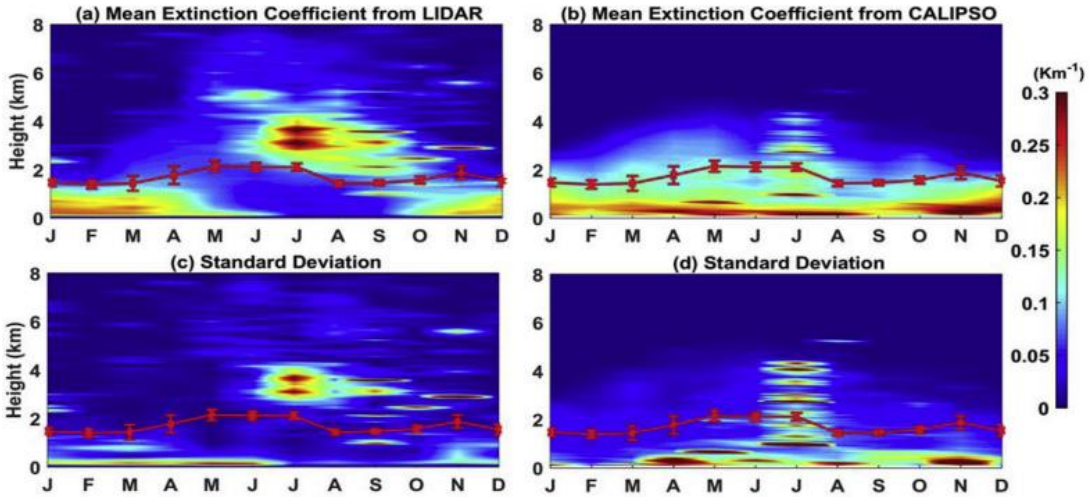

Fig. 3. Monthly mean variation of aerosol extinction observed by (a) NARL/SVU Lidars and (b) CALIPSO averaged during 2010-2017. Corresponding standard deviations are shown in (c) and (d), respectively. Red line and vertical bars shows the ABL altitude and standard deviation obtained from radiosonde launched from 2010 to 2017.

(iv) Monitoring of Atmospheric Parameters Using GPS-RO Techniques.

Diurnal and seasonal variation of surface anomalous wave propagation parameters like surface refractivity (Ns), initial refractivity lapse rate (ILR) and earth curvature factor (k) are presented across the globe using 9 years of Constellation Observing System for Meteorology Ionosphere and Climate (COSMIC) GPS RO measurements. Profiles reaching down to 0.2 km are only considered for the analysis. Number of profiles reaching to surface over oceans is maximum compared to the land regions. Compared to other regions, the occultations reaching down to 0.2km are observed maximum (350-500) over mid latitudes. Spatially, Ns is found maximum (320-380 N-units) over equatorial latitudes covering mostly over the oceans and it is minimum over the desert regions of Africa, Australia, west coast of North and South America, Himalayan and Afghanistan regions. ILR has also been found to be large (60 N-units/km) in the equatorial latitudes and minimum (20 N-units/km) over above mentioned locations. k seems to be maximum (0.9) over land region especially in the desert areas of Africa and Australia compared to that over ocean and it is observed to be minimum over west coast of North America, South America and Africa. No significant day and night variation in the Ns, ILR and k is noticed over the ocean regions but it is large over land regions. Over the African region, Ns, ILR and k is high during nighttime but quite opposite features have been noticed over Australian region. These surface

variations are expected to have direct effect on the temporal and spatial variation of duct characteristics and hence anomalous radio wave propagations.

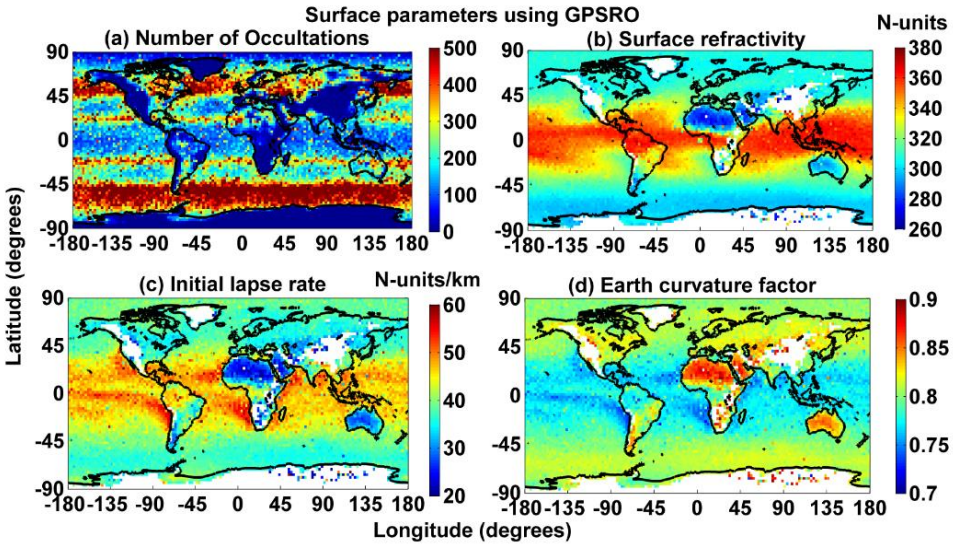

Fig. 4. Latitude and longitudinal variation of (a) number of COSMIC GPS radio occultations reaching down to 0.2 km, (b) surface refractivity, (c) initial refractivity lapse rate and (d) earth curvature factor averaged during 2006 to 2014.

(v) Prediction of Rainfall (inclusive of Monsoon and tropical cyclones) and High impact Weather Events over India Using High Resolution Weather Prediction Models.

Extreme rainfall events pose a serious threat of leading to severe floods in many countries worldwide. Therefore, advance prediction of its occurrence and spatial distribution is very essential. In this paper, an analysis has been made to assess the skill of numerical weather prediction models in predicting rainstorms over India. Using gridded daily rainfall data set and objective criteria, 15 rainstorms were identified during the monsoon season (June to September). The analysis was made using three TIGGE (THe Observing System Research and Predictability Experiment (THORPEX) Interactive Grand Global Ensemble) models. The models considered are the European Centre for Medium-Range Weather Forecasts (ECMWF), National Centre for Environmental Prediction (NCEP) and the UK Met Office (UKMO). Verification of the TIGGE models for 43 observed rainstorm days from 15 rainstorm events has been made for the period 2007–2015. The comparison reveals that rainstorm events are predictable up to 5 days in advance, however with a bias in spatial distribution and intensity. The statistical parameters like mean error (ME) or Bias, root mean square error (RMSE) and correlation coefficient (CC) have been computed over the rainstorm region using the multi-model ensemble (MME) mean. The study reveals that the spread is large in ECMWF and UKMO followed by the NCEP model. Though the ensemble spread is quite small in NCEP, the ensemble member averages are not well predicted. The rank histograms suggest that the forecasts are under prediction. The modified Contiguous Rain Area (CRA) technique was used to verify the spatial as well as the quantitative skill of the

TIGGE models. Overall, the contribution from the displacement and pattern errors to the total RMSE is found to be more in magnitude. The volume error increases from 24 hr forecast to 48 hr forecast in all the three models.

Using a high-resolution daily gridded rainfall data set for the period 1951–2015, new objective criteria were developed to determine rainstorms over the Indian region during the south-west monsoon season (June to September). The rainstorms thus identified have rainfall of 125 mm/day or more at the centre, cover minimum 50,000 km2 in area with rainfall of 25 mm or more and sustain for at least two consecutive days. These rainstorms have potential to cause large-scale floods and associated risk over the region in which they are present. The analysis identified 395 rainstorms during the period, 1951–2015, on an average 6 storms per season. About 40% of the rainstorms are associated with the low-pressure systems which form over the North Bay of Bengal and move northwest wards along the seasonal monsoon trough. The present analysis suggests that over northern parts of India, where majority of rainstorms form, frequency and duration of rainstorms have shown statistically significant increasing trends. During the period of 1951–2015, there was an increase from 4 to 8 rainstorms per year and from 12 to 27 rainstorm days per year. This increase has significant repercussions in terms of added risk of large-scale floods and associated causalities. Further analysis suggests that rainstorm activity over northern parts of India is strongly influenced by the colder sea surface temperature anomalies over the east equatorial Indian Ocean and associated moisture divergent flow and strong moisture convergence over the Indian landmass and the Bay of Bengal.

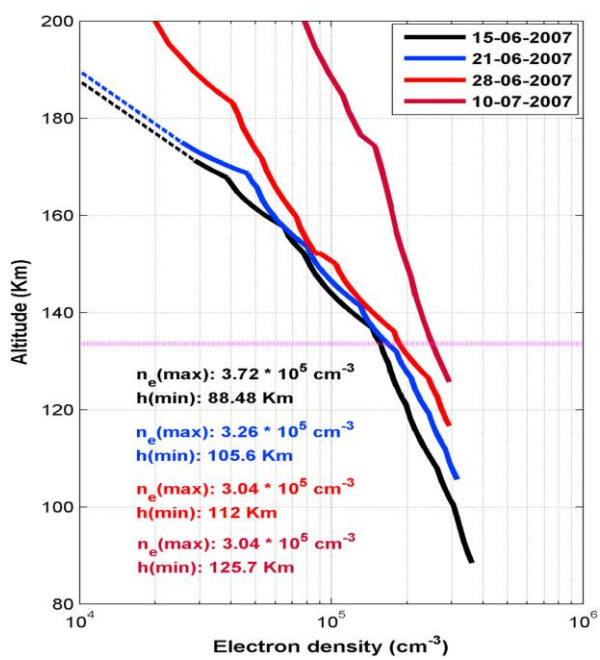

Fig. 5 Frequency of heavy rainfall events (rainfall >125 mm/day) during the monsoon season for the period June to September, 1951-2015. The area (box) considered to prepare time series of rainstorms and rainstorm days is also shown.

I. Studies on Enhanced Ionization in Magnetic Anomaly of Martian Lower Ionosphere Associated with Dust Storm:

The Mars Advanced Radar for Subsurface and Ionospheric Sounding instrument aboard the Mars Express spacecraft observes vertical echoes from the normal ionosphere and oblique echoes from ionization bulges. The peak frequencies of these two kinds of echoes are, in general, nearly equal. In the present study, we report the detection of oblique echoes whose peak frequencies are much larger than those of the vertical echoes. Figure1 shows oblique echoes were observed on 15 June, 21 June, 28 June, and 10 July 2007, respectively. All these oblique echoes were observed from a region of strong crustal magnetic fields. Figure 2 shows dispersion corrected electron density profiles observed on 15, 21 and 28 June and 10 July of 2007, the maximum electron density in the first case is found to be 3.75 × 105 cm^{-3} and is observed at an altitude of ~88 km. In subsequent cases, a gradual decrease in peak electron density and an increase in altitude are observed. The causative mechanism of these oblique echoes is examined by considering various forces from top and bottom. During the times of the observations, there were no solar flares or meteor in fall.

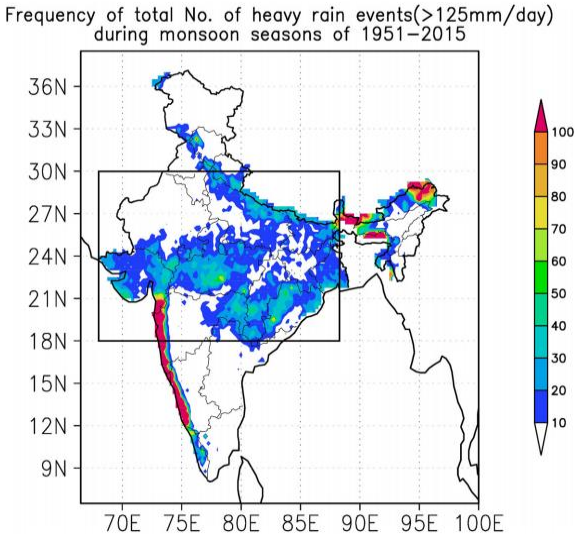

Figure 1. A series of five ionograms from each of the orbits (left to right) observed on 15 June, 21 June, 28 June, and 10 July 2007 showing the strong oblique echoes and their change in separation with the vertical echoes. The red arrows in the middle panels mark the peak frequencies of the merged echoes. The presence of solar energetic particles also could not be firmly established. We found that these strong oblique echoes were observed at the initial phase and during the progression of a planet-encircling dust storm in Martian Year 28. Similar, but weaker features were observed in other dust storm seasons as well. Mechanisms causing such oblique echoes in the regions of strong magnetic field.

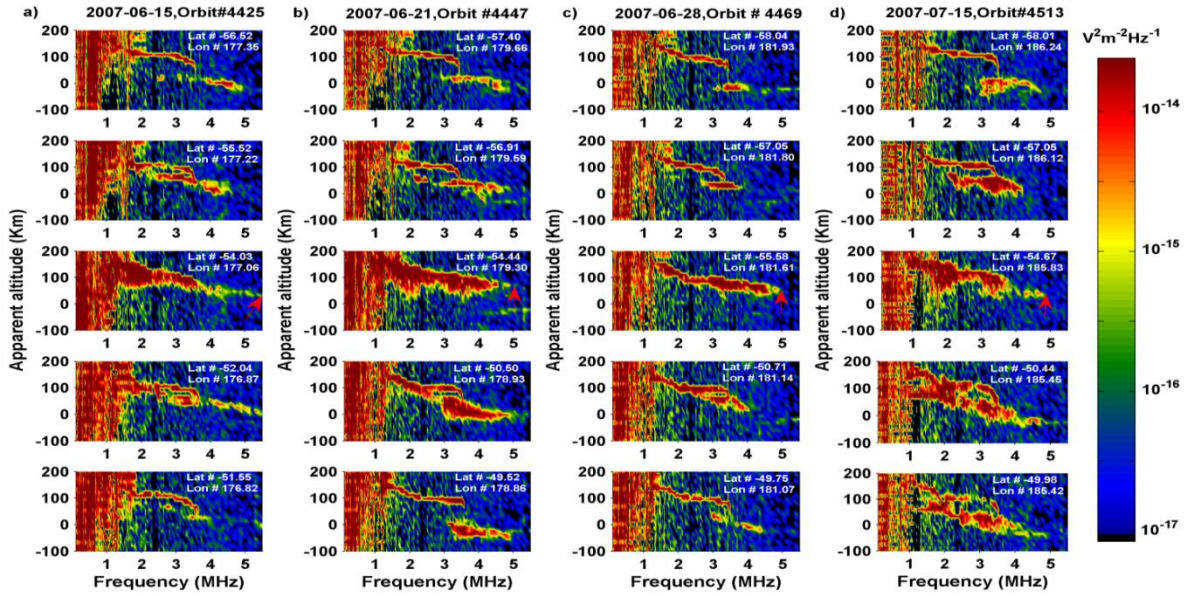

Figure 2 Dispersion corrected electron density profiles of Mars Advanced Radar for Subsurface and Ionospheric Sounding oblique echoes observed on 15, 21, and 28 June and 10 July 2007. The dashed black and blue lines are due to interpolation of the electron density profiles between the density at the spacecraft and that of the lowest sounding echo. The dotted horizontal line represents the altitude of the normal ionosphere obtained from Němecet al. (2011) for the observed conditions.

II. Isolated High Density Structures in Magnetic Anomaly Regions of the Martian Lower Ionosphere

The occurrence of density structures in magnetic anomaly regions is one of the prominent features of the Martian ionosphere. These structures, in general, occur at altitudes above the main peak. In this paper, we analyse four cases of unusually strong oblique echoes that occur in magnetic anomaly regions and are observed by the Mars Express MARSIS instrument from (VenkateswaraRao et al 2019). An in-depth analysis suggests that these strong oblique echoes, in fact, correspond to the density structures. After correcting for dispersion effects these structures are found to occur in the lower ionosphere at altitudes as low as 88 km. Figure1 shows ray propagation simulations carried out in this study demonstrate that the density structures can be modeled as Gaussian shapes distributed along planetary latitude. The density of these structures decreases with an increase in altitude. Accordingly, Figure2 shows the density structures at higher altitudes are associated with iso-density contours of the background ionosphere. In the lower ionosphere, however, the density structures are found to immerse in a background ionosphere whose density is much smaller than those of the density structures. The possible causes and

consequences of such low altitude density structures are discussed. The results of this study are combined with those of previously reported studies to produce a comprehensive picture of these magnetically controlled density structures.

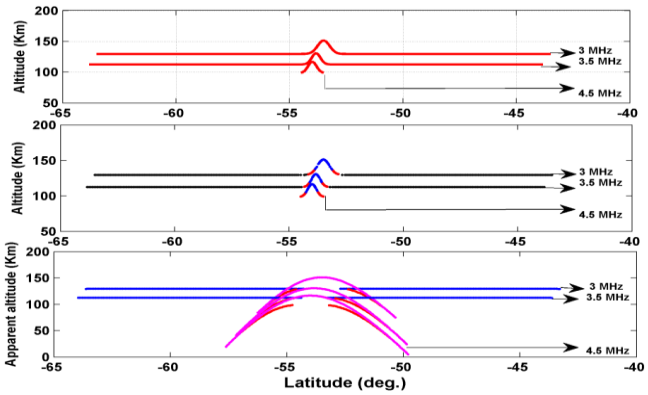

Figure 1 (Top panel) the modeled Gaussian bulges that correspond to the normal ionosphere and the high density structures. (Middle panel) various reflection points on the bulge; black represents the reflections from the stratified ionosphere, red represent those from the ascending slope elevations of the bulge, and blue from the surrounding regions of apex of the bulge. The bottom panel represents the echograms resulting from the Gaussian bulges; blue for the vertical echoes and magenta and red for the oblique echoes.

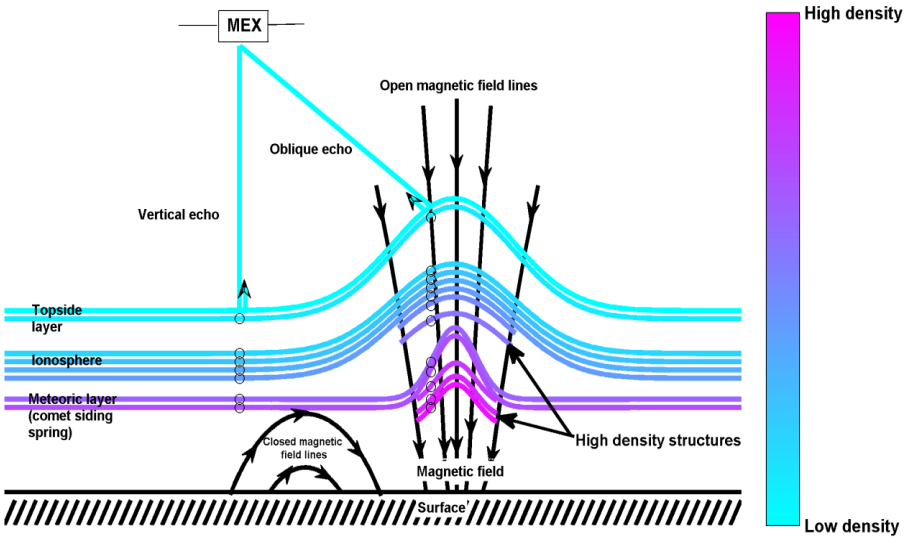

Figure 2 A schematic diagram showing the magnetically controlled density structures at multiple altitudes constructed from the results of the present study and those from the published literature.

III. Nocturnal, seasonal and intra-annual variability of tropospheric aerosols observed using ground-based and space-borne Lidars over a tropical location of India:

The clear sky aerosol extinction profiles obtained from the MPL observations at SVU and NARL are combined to obtain the seasonal mean profiles as shown in Figure1. In addition, the seasonal mean CALIPSO extinction profiles over the grid box (12°N-14°N & 77.5°E- 82.5°E) covering both the observation sites is included in the respective panels. In order to investigate the influence of Lidar Ratio (LR) on the magnitude of MPL-derived aerosol extinction over this location, we have derived aerosol extinction for different LR values namely, 20, 40 and 70 sr and superimposed with CALIPSO-derived aerosol extinction for each season. It should be noted that based on the evaluation of CALIPSO's 532 nm LR selection algorithm using AERONET Sun Photometers (Lopes et al., 2013), the aerosol types are classified into: Desert Dust (40+20 sr), Smoke/Biomass Burning (70+28 sr), Clean Continental/Background (35+16 sr), Polluted Continental (70+25 sr), Clean Marine (20+6 sr), and Polluted Dust (55+22 sr).

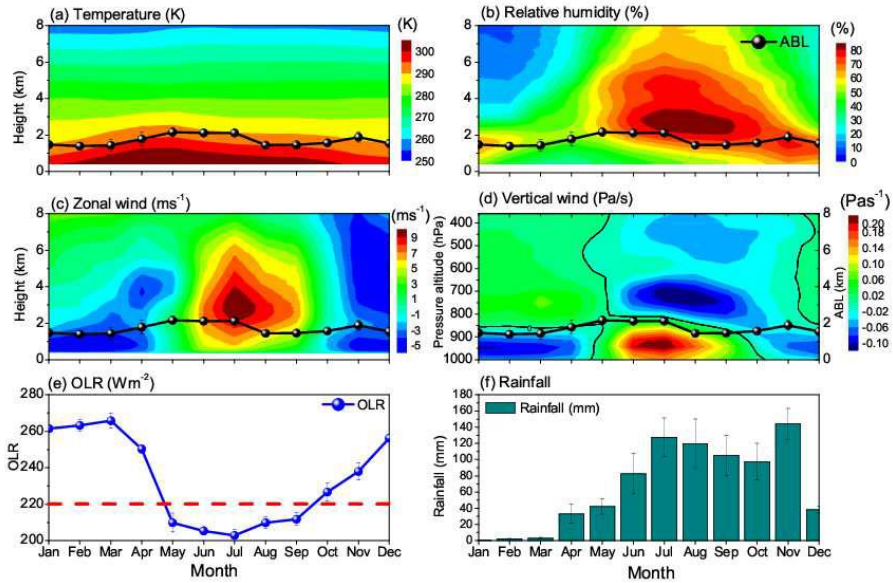

Figure 1 Composite monthly mean (a) temperature, (b) relative humidity, (c) zonal wind observed using GPS radiosonde measurements over Gadanki averaged during 2010 to 2017. ABL altitude obtained from radiosonde measurements is also superimposed (black line with solid circle). (d) Composite monthly mean vertical wind obtained from ERAInterim data averaged during 2010 to 2017. (e) Gridded composite monthly mean OLR (blue line with solid circle) and (f) Monthly mean accumulated rainfall over Gadanki during 2010 to 2017.

The MPL extinction profiles of winter (Figure1a) and post-monsoon (Figure 1d) seasons showed higher extinction values within 2 km altitude, and relatively low in the higher altitudes. This feature is mainly attributed to the persistence of lower ABL altitudes (< 2 km) and lower wind speed as shown in Figure 1c. High OLR during these seasons indicate less convection (Figure 1e) at the surface but there exist updrafts within the boundary layer due to the presence of rising branch of normal Hadley circulation as discussed in Roja Raman et al. (2008) over this region. Sinha et al. (2013) also reported that the shallow boundary layer and low wind speeds during winter and post-monsoon season results in the accumulation of more pollutants including black carbon aerosols near the surface level. The CALIPSO extinction profiles superimposed on MPL observations shows a close match with each other both in trend as well as magnitude of aerosol extinction during winter (~ 0.25 km-1) and post monsoon (~ 0.3 km-1) season. During summer season, most of the aerosols are distributed from surface to higher altitudes of about ~5 km as shown in Figure 1b.

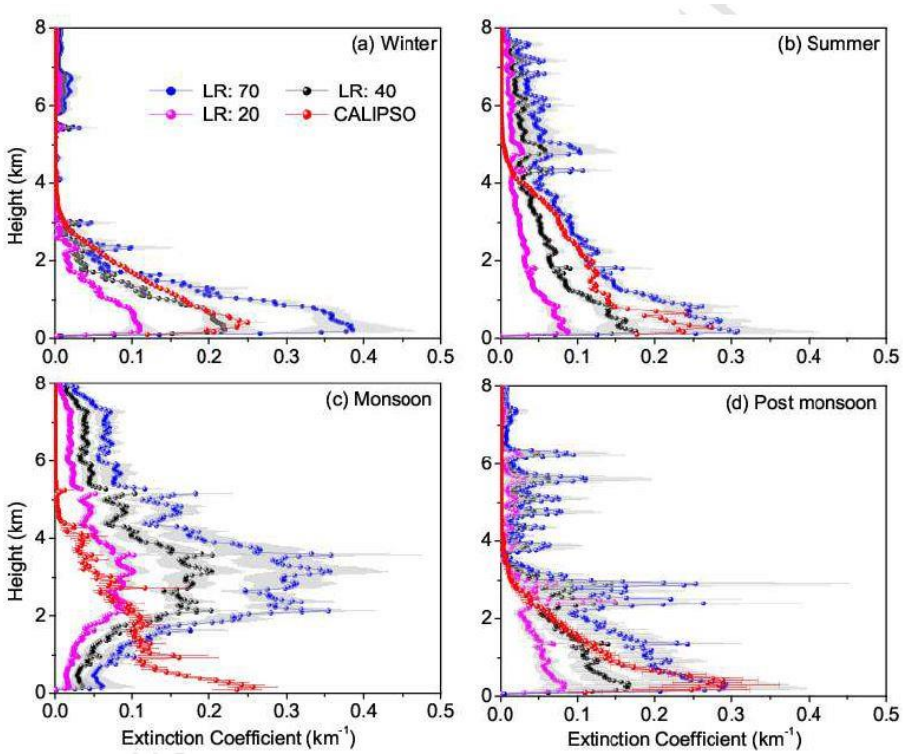

Figure2 Composite **s**easonal mean of aerosol extinction coefficient (km-1) obtained from combined SVU and NARL-MPLs using different LR values during (a) winter, (b) summer, (c) monsoon and (d) post-monsoon. Seasonal mean profiles obtained from CALIPSO are also superimposed in the respective panels. The horizontal bar corresponds to standard error.

During this season, enhanced insolation at the Earth's surface especially during clear sky days results in higher air temperature (Figure 1a) and deepening of the ABL height than other seasons. Hence, strong vertical mixing due to enhanced turbulence advects surface aerosols to higher altitudes (Gautam et al., 2009). In addition, the vertical wind from ERA data (Figure 1d) shows an upward motion during summer.

The CALIPSO-derived mean extinction profile also extend upto ~5 km and concur with MPL extinction profile obtained with a Lidar ratio (LR) of 70 sr but not with LR of 40 sr during this season. A gradual decrease in the extinction at higher altitudes is clearly noticed in both the observations, but the MPL-derived aerosol extinction with LR of 20 sr is close to CALIPSO-derived aerosol extinction (Figure2b). This indicates the varying aerosol type with altitude. It should be noted that CALIPSO adopts a range-dependent LR while retrieving aerosol extinction profiles, but we have used constant LR in our algorithm that might be the reason for this discrepancy between two observations at different heights. If the range-dependent LR is adapted to MPL retrieval, both observations may show exact aerosol extinction profiles.

During monsoon season, the MPL-derived aerosol extinction profile is quite differentfrom the other seasons over this region. The higher extinction values (~0.2 km-1) are found above ~2 km up to 5.5 km and very low extinction (~0.05 km-1) near to the surface. In contrast, CALIPSO-derived aerosol extinction values are high (~0.25 km-1) near the surface and decreases slowly up to 5 km in this season. Both CALIPSO and MPL derived aerosol extinction profiles are coinciding well above 2 km altitude for LR of 20 sr during monsoon season. Whereas, in post monsoon season the MPL-derived aerosol extinction profile below 1 km altitude with a LR of 70 sr matches well with that of CALIPSO. Above 1 km, the CALIPSO-derived aerosol extinction profile matches with the MPL aerosol extinction derived with a LR of 40sr (Figure2d). It is clearly evident that the range-dependent LR or simultaneous sun photometer measurements are required to improve the retrieval of aerosol extinction profiles from MPL in comparison with CALIPSO retrievals.

1. Disrupted Stratospheric QBO Signatures in the Diurnal Tides Over the Low-Latitude MLT Region

Meteor radar measurements of winds in the mesosphere and lower thermosphere (MLT)over Tirupati (13.63°N, 79.4°E; 2013–2020) and Microwave Limb Sounder (MLS) observations of ozoneare used for investigating the effect of the disrupted stratospheric quasi-biennial oscillation (SQBO)during the year 2016 on the diurnal tides. The positive tidal perturbations are observed during positiveperturbations of ozone and eastward phase of the SQBO and vice versa. These observations are wellcaptured by the Specified Dynamics Whole Atmosphere Community Climate Model (SD-WACCM)simulations.

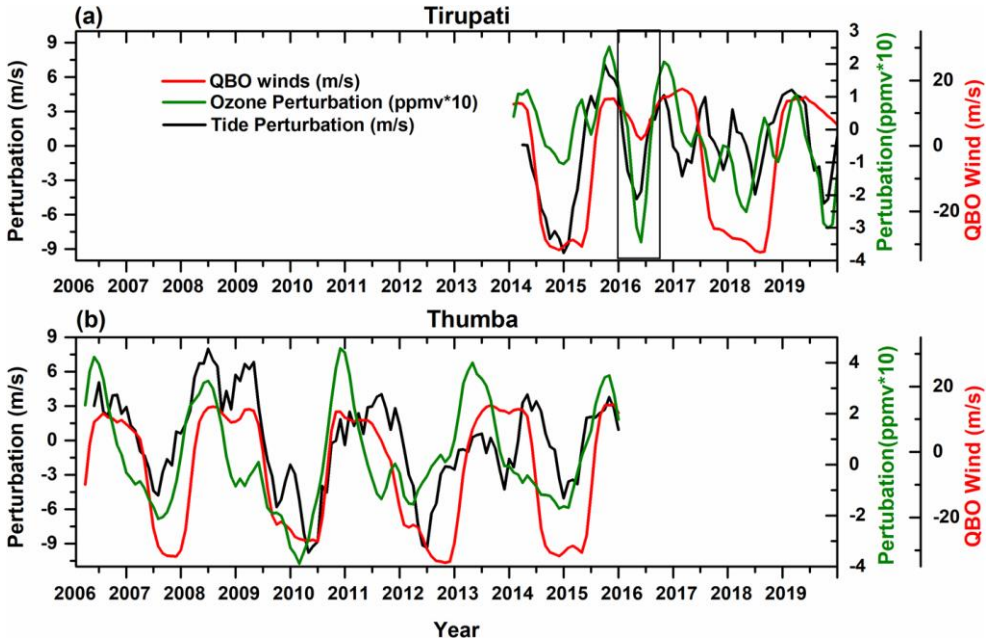

Fig.1 Interannual variability of deseasonalized diurnal tide perturbations in the meridional winds at 88 kmaltitude derived from meteor radar observations (black), SQBO winds (red) at 30 hPa level and deseasonalizedozoneperturbations (green) at 26 hPa over (a) Tirupati and (b) Thumba.

During the year 2016, for the first time the SQBO disruption took place. The present study investigates the effect of the SQBO disruption on the amplitudes of the diurnal tides in the MLT region using meteor radar observations over a low-latitude station. Stratospheric ozone

measurements obtained from Microwave Limb Sounder (MLS) as well as simulations from Specified Dynamics Whole Atmosphere Community Climate Model (SD-WACCM) are also employed to shed light on the relation among diurnal tides, SQBO winds and ozone shown in Fig. 1. The results suggest a positive correlation between diurnal tide perturbations and ozone perturbations as well as SQBO winds. During the SQBO disruption, there is a negative anomaly in the ozone perturbations and westward winds below 20 hPa, which are thought to be the prime candidates inreducing the observed diurnal tide amplitudes in the MLT.Atmospheric tides are global scale oscillations with periods that are sub-harmonics of a solar day (24, 12, 8 h etc.). Among these, diurnal tides (24 h) are very prominent over low latitudes and play a major role in shaping the structure and dynamics of the middle atmosphere. Stratospheric quasi-biennial oscillation (SQBO) is a long period oscillation with a mean time period of ∼28 months in the stratosphere and is believed to modulate diurnal tides at interannual time scales.

2. Variability of temperatures and gravity wave activity in the Martian thermosphere during low solar irradiance

This present work deals with temperatures and gravity wave (GW) activity in the Martian thermosphere during low solar activity. For this purpose, we extracted the GW amplitudes and thermospheric temperatures from CO2 densities measured in situ by the Neutral Gas and Ion Mass Spectrometer (NGIMS) aboard the Mars Atmosphere and Volatile EvolutioN (MAVEN) mission. These observations were obtained during the declining phase of solar activity between solar longitude (Ls) =294° in Mars year (MY) 32 and Ls = 242° in MY 35. The observations of the present study show that the temperatures are lower and GW amplitudes are higher at low solar activity. The response of the thermospheric temperatures to solar irradiance is local time dependent such that the noontime and duskside temperatures show significant correlation (correlation coefficient, R > 0.8) with the solar irradiance whereas the temperatures on the dawnside show moderate correlation (R = 0.55) shown in Fig. 2. Furthermore, the nominal negative correlation between the gravity wave amplitudes and thermospheric temperatures, which was disturbed during the 2018 global dust event, was restored after the subsidence of the event.Interestingly, the correlation between the thermospheric temperatures and GW activity is also local time dependent with moderate correlation at noon (R = -0.65) and weak correlation at other local times shown in Fig.3.

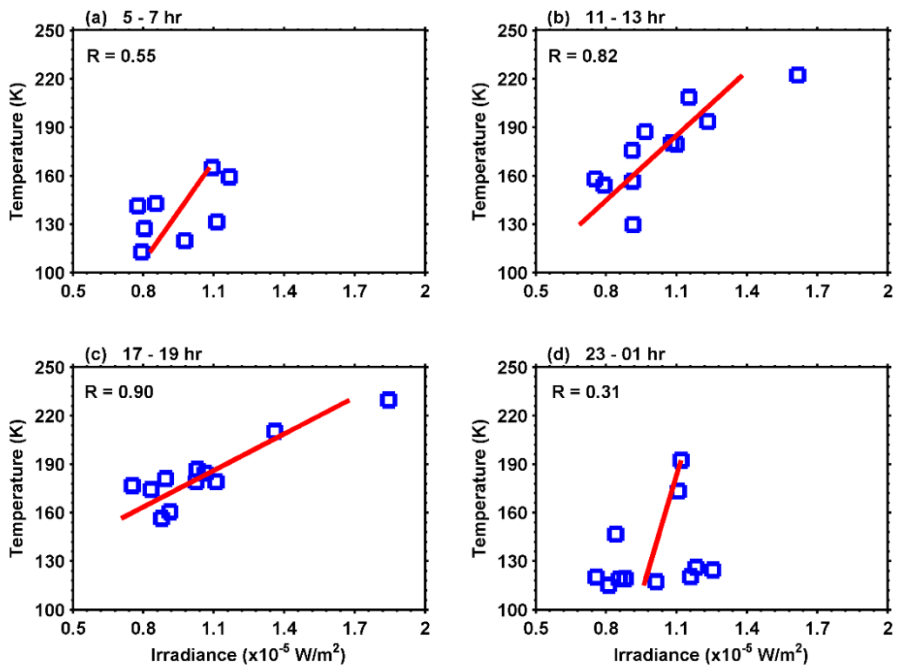

Fig.2 Scatter plot between solar irradiance and thermosphericterperature depicting the correlation coefficient (a) 5 – 7 h (b) 11 – 13 h (c) 17 – 19 h (d) 23 – 01 h. The solid red line shown the best fit for each dataset.

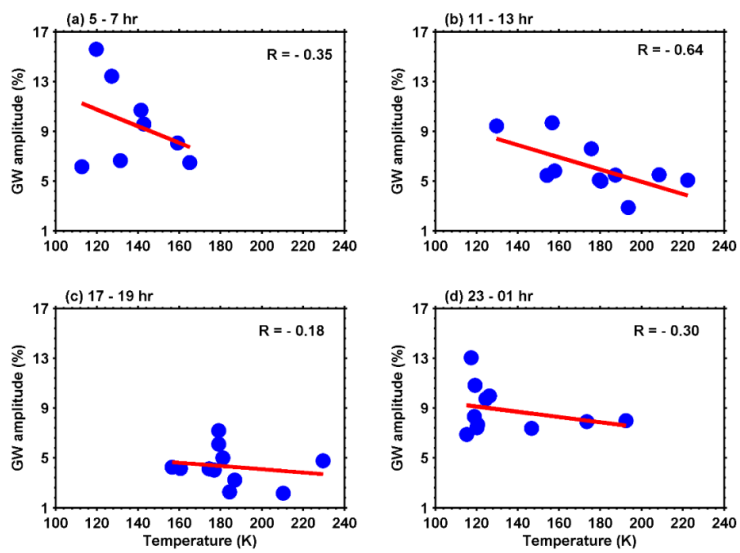

Fig.3 Same as **Fig.2**, but shows the correlation analysis between the thermospheric temperature and GW activity.

From the results of the present study, it is inferred that the variability of GW amplitudes in the Martian thermosphere are not necessarily controlled by the temperatures of the underlying atmosphere alone. Other factors, such as the variation of GW amplitudes at the source region and/or changes in the circulation of the underlying atmosphere, are also likely to play a significant role, particularly at the terminator and on the nightside.

IV. Performance Optimization of Operational WRF Model Configured for Indian Monsoon Region

To find out the suitable combination of the computed nodes and number of cores per node using the Indian benchmark on UGC HPC, we first conducted scalability experiments by varying both the number of computed nodes from 20 to 100 as well as the number of cores in the compute node shown in Figure 1(b). The performance bar shown in Figure 1(b) is plotted with the computational time taken in minutes to complete the model forecast of 72 h against the nodes including the number of cores. The computational time reported in this study is calculated by neglecting the time taken for input/output (IO) and model initialization, and also the results presented are with six sets of cores/processor combinations per node (4, 8, 10, 12, 14 and 16 per node). The scalability results suggest that the WRF model with configured domain can scale up to 960 cores in logarithmic manner; however, 480 cores (12 cores and 40 nodes) itself provide the optimize performance. It is also noticed that with increasing number of cores per node, the computing time is decreasing and the input/output (IO) writing time is increasing. Model exhibits a strong scalability observed up to 40 compute nodes, a weak scalability until 60 compute nodes, thereafter the scalability reaches saturation point (particularly after 80 compute nodes). After 80 compute nodes, simulation time follows a negative trend as the time is increasing instead of decreasing. Also we observed that by increasing the number of processes per node, strong scalability is coming down.We have performed four types of simulations by Varying Cloud Microphysics (CMP) schemes, namely WSM3 (WRF-single-moment microphysics class 3), WSM6 (WRF-single-moment microphysics class 6), Thompson (Thompson et al. 2008) and New Thompson Schemes. Figure 2 (a) shows the scalability analysis performed by plotting the time taken for four CMP schemes by increasing the number of nodes to simulate 72-hour model forecasts. The results clearly show that the time taken for completing 72-hour simulation increases with complexity of CMP and the maximum time taken is found to be high in the case of New Thompson scheme.

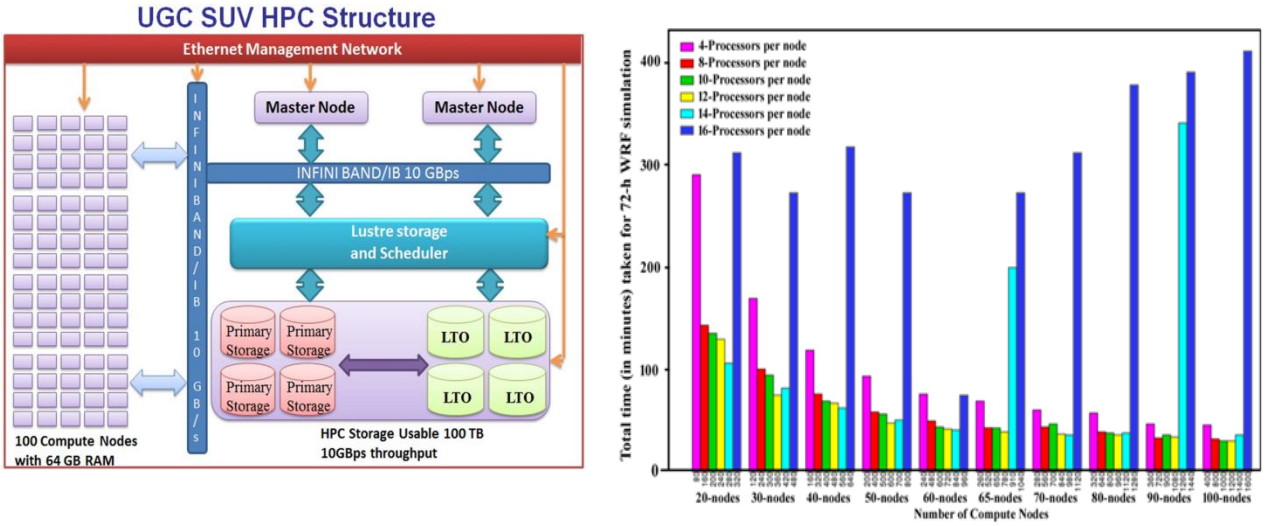

Figure: 1 (a) A generic block diagram of UGC S.V University HPC (b) Scalability analysis of WRF plotted with the computational time taken by operational workflow (in minutes) against the number of computational nodes.

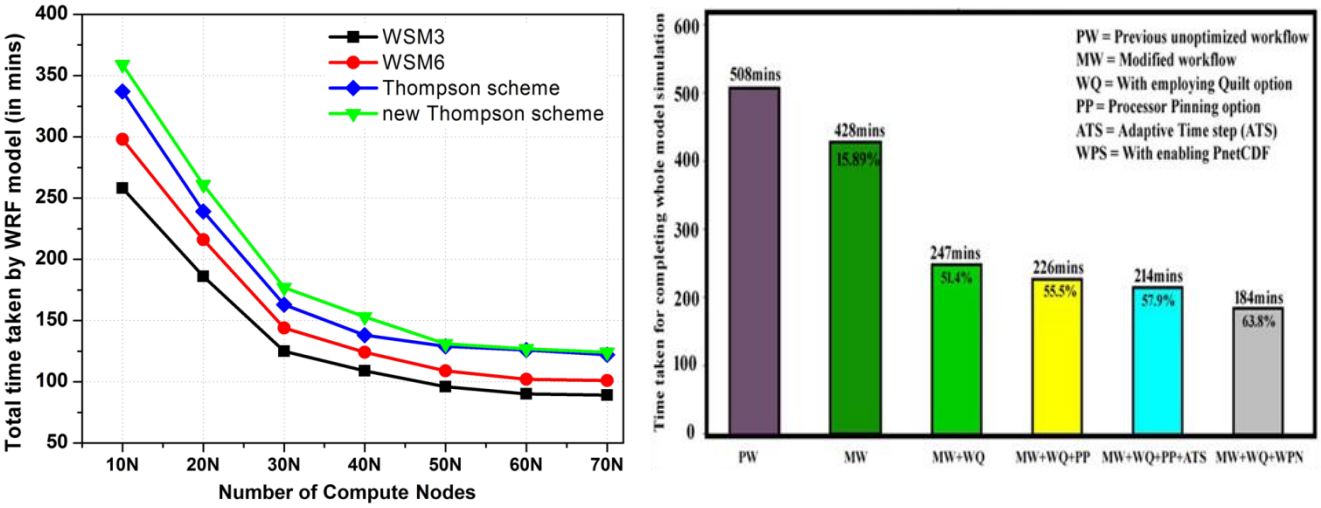

Figure 2 (a) Variation of computational time taken by the four microphysical schemes to complete 72-hours forecast against the number of computational nodes (b) The effect of different IO optimizations on the total time taken by the operational model.

Though the large differences in the computational time found with less number of computational nodes, when the model reaches saturation point the time differences are reduced drastically in all

the schemes. The computational times in all schemes remain constant when we use relatively sufficient number of computational nodes. This also reflects that though the complex CMP is configured for your operational setup, the complex representation may not have high impact on the total computational time taken by the model when we use large number of nodes.

Selected List of Publications During (2017-2021):

1. Venkateswara Rao, N., P. MohanaManasa, and **S. V. B. Rao** (2017), Magnetically controlled density structures in the topside layer of the Martian ionosphere, *J. Geophys.Res. Space Physics*, 122, doi:10.1002/2016JA023545. **Impact factor: 3.426**
2. KarunaSagar, S., Rajeevan, M. &**VijayaBhaskara Rao, S**. (2017), On increasing monsoon rainstorms over India, *Nat Hazards*, 85: 1743. doi:10.1007/s11069-016-2662-9. **Impact Factor: 1.746**
4. S. KarunaSagar, M. Rajeevan, **S. VijayaBhaskara Rao**, A.K. Mitra (2017), Prediction skill of rainstorm events over Indiain the TIGGE weather prediction models, Atmospheric Research, 198,194-204.
5. S**.** KarunaSagar, G. Mrudula, K. Vijaya Kumari**, S. Vijaya Bhaskara Rao, (**2017), Verification of VARSHA Rainfall Forecasts for Summer Monsoon Seasons of 2009 and 2010, Int J Cur Res Rev,9,21
6. Prasad P, M. Rojaraman, M. VenkatRatnam, Wei-Nai Chen, **S. Vijaya BhaskaraRao**, M. M. Gogoi, K. Sobhan Kumar, S Suresh Babu, K. Sarat. Characterization of atmospheric Black Carbon over a semi-urban site of southeast India: Local sources and long-range transport. Atmospheric Research, 213 (2018) 411-421. **Impact factor: 3.78**

7. Vijayakumar, K., Devara, P. C. S., Sonbawne, S. M., Giles, D. M., Holben, B. N., **S Vijaya Bhaskara Rao** and Jayasankar, C. K.: Solar radiometer sensing of multi-year aerosol features over a tropical urban station: Direct Sun and inversion products, Atmos. Meas. Tech. Discuss., https://doi.org/10.5194/amt-2019-437, in review, 2019.K Pradhan, Margarida LR Liberato, Vinay Kumar, S Vijaya Bhaskara Rao, Juan Ferreira, TusharSinha (2019).

8. P Mohanamanasa, N Venkateswara Rao, V Leelavathi**, S Vijaya Bhaskara Rao (2019)** Isolated High-Density Structures in Magnetic Anomaly Regions of the Martian Lower Ionosphere, Journal of Geophysical Research: Space Physics, 124,**pp 6296-6304**. **Impact Factor:2.82.**
9. P Prasad, M Roja Raman, M VenkatRatnam, V Ravikiran, BL Madhavan, **S Vijaya Bhaskara Rao, (2019).** Nocturnal, seasonal and intra-annual variability of tropospheric aerosols observed using ground-based and space-borne lidars over a tropical location of India, Atmospheric Environment.213, pp 185-198.**Impact Factor: 4.012**

10. N Venkateswara Rao, V Leelavathi, P Mohanamanasa, SA Haider, **S Vijaya Bhaskara Rao, (2019).**Enhanced ionization in magnetic anomaly regions of the Martian lower ionosphere associated with dust storms, Journal of Geophysical Research: Space Physics124,pp3007-3020:**Impact Factor:2.82.**

11. PavaniAndraju, A Lakshmi Kanth, K Vijaya Kumari, **S Vijaya Bhaskara Rao (2019)** Performance Optimization of Operational WRF Model Configured for Indian Monsoon Region, Earth Systems and Environment, 3, pp 231–239. **Impact Factor:8.20**
12. V Ravi Kiran, M VenkatRatnam, BV Krishna Murthy, Yogesh Kant, P Prasad, M Roja Raman, **S Vijaya Bhaskara Rao,** TV Lakshmi Kumar, AnimeshMaitra,(2019). An empirical method for source apportionment of black carbon aerosol: Results from Aethalometer observations at five different locations in India, Environmental Pollution,254,pp112932, **Impact Factor:5.950**
13. Kishore Pangaluru, Isabella Velicogna, YaraMohajerani, Enrico Ciracì, SravaniCharakola, GhouseBasha, **S Vijaya Bhaskara Rao** (2019). Soil Moisture Variability in India: Relationship of Land Surface–Atmosphere Fields Using Maximum Covariance Analysis, Remote sensing, 11, pp335-**Impact Factor: 4.118.**
14. Manjula. G., M. Roja Raman, M. VenkatRatnam, A.V. Chandra Sekhar and **S.VijayaBhaskara Rao (2019).** Diurnal and Seasonal variation of surface anomalous wave propagation parameters (Ns, ILR and k) observed using COSMIC GPS RO measurements, Radio Science, 2018RS006697 (Revision submitted) **Impact Factor: 1.45**.**Impact Factor: 2.177.**
15. S Eswaraiah, KondapalliNiranjan Kumar, Yong Ha Kim, G VenkataChalapathi, Wonseok Lee, Guoying Jiang, Chunxiao Yan, Guotao Yang, M VenkatRatnam, P Vishnu Prasanth, SVB Rao, K Thyagarajan**(2020),** Low-latitude mesospheric signatures observed during the 2017 sudden stratospheric warming using the fuke meteor radar and ERA-5, Journal of Atmospheric and SolarTerrestrial Physics, **Impact Factor: 1.503**.
16. Kavutharapu, Renuka&Gadhavi, Harish &Achuthan, Jayaraman& Vijaya Bhaskara Rao, S. &Lal, Shyam. **(2020)**. Study of mixing ratios of SO2 in a tropical rural environment in south India. Journal of Earth System Science. 10.1007/s12040-020-1366-4. Volume 129.**Impact Factor:1.423.**
17. V Leelavathi, N Venkateswara Rao, **SVB Rao,(2020).** Interannual variability of atmospheric gravity waves in the Martian thermosphere: Effects of the 2018 planet-encircling dust event, Journal of Geophysical Research: Planets, 125, e2020JE006649. 10.1029/2020JE006649. **Impact Factor: 3.72.**
18. Rambabu. G., Prasad. P., Raman, M.R. Ratnam, M.V., S. Vijayabhaskara Rao. (2020). Long- term changes in land surface temperature due to land use land cover over a mega city in south India, The journal of India, The Journal of Indian Geophysical Union, 24(6), 1-14, **Impact Factor**: 0.313.
19. LatitudesM. Pramitha[1], K. Kishore Kumar, M. VenkaRatnam, M. Praveen, and **Prof. S. Vijaya Bhaskara Rao**.(2021).Stratospheric Quasi Biennial Oscillation Modulations of

Migrating Diurnal Tide in the Mesosphere and Lower Thermosphere Over the Low and Equatorial, JGR Space Physics, Doi:10.1029/2020JA 028970, **Impact Factor**:0.19.

20. Maosheng He, Jorge L. Chau, Jeffrey M. Forbes, Xiaoil Zhang, Christoph R. Englert, Brian J. Harding, Thomas J. Immel, LourivaldoM.Lima, **S. Vijaya Bhaskara Rao,** M. VenkaRatnam, Guozhu Li, John M. Hardlander Kenneth D, Marr, and Jonathan J. Makela.(2020).Quasi-2-Day Wave in Low- Latitude Atmospheric Winds as Viewed From the Ground and Space During January, March, 2020, Geophysical Research Letters, Doi: 10.1029/2021GL093466, **Impact Factor**:4.72.

Seminar/ Workshops/ Conferences Organized:

1. Recent Advances In Observations And Data Assimilation Techniques For Severe Weather Prediction, 23-24, March 2017:

On the occasion of World Meteorological Day, UGC-SVU Centre for MST Radar applications, Dept. of Physics, S.V. University has organised a twoday workshop on "Recent advances in observations and data assimilation techniques for severe weather forecasting"during 23-24 March.*Prof.A.Damodaram, VC SVU has inaugurated the workshop.*This workshop was aimed for the young scholars and faculty working in the field of atmospheric sciences to give a touch on short-range weather forecasting tools and effective utilization of Satellite data towards the improvement of the weather prediction.

2. A Two Day National Level Workshop on **"HANDS ON DESIGN AND SIMULATION OF PROGRAMMING ON EMBEDDED – C"** held on 7-8 September, 2019 in the Department of Physics, SV University, Tirupati. (**125** Students participated).

3. A Two Day National Level Workshop on **"PCB DESIGNING & FABRICATION"** held on 14-15 September, 2019 in the Department of Physics, SV University, Tirupati. (**100** Students participated).

4. A Two Day National Level Workshop on **"EMBEDDED SYSTEMS USING ARM 7"** held on 19-20October,2019 in the Department of Physics, SV University, Tirupati. (**100** Students participated).